Third Semi-Annual
Progress Report

To: National Aeronautics and Space Administration
Goddard Space Flight Center
Greenbelt, Maryland 20771

Contract: NAS5-28758

Title: Spectral characteristics and the extent of paleosols of the Palouse formation

Principal Investigator: Dr. B. E. Frazier
Agronomy and Soils
Washington State University
Pullman, WA 99164

Collaborators: Dr. Alan Busacca

Yaan Cheng
Agronomy and Soils

David Wherry

Judy Hart

Steve Gill
Digital Image Analysis Laboratory

Introduction

The third six month period of our work has been devoted to analysis of image data and verification by comparison to previously gathered transect samples and to aerial photographs. We report work by objective as stated in our proposal.

Progress by Objective:

I.A. Develop spectral relationships from TM data that will define the spatial distribution of soil areas by levels of (1) organic matter in the surface soil, (2) iron oxide and clay in exposed paleosol B horizons, and (3) lime-silica accumulations in exposed paleosol B horizons.

B. Compare areas determined by the method outlined in A to patterns interpreted from color aerial photographs, and to ground observations on bare-soil fields.

In this reporting period we have investigated a bare-soil field with exposed paleosols characterized by slight enrichment of iron. Spectral relationships were first investigated statistically by creating a data set with DN values spatially matched as nearly as possible to field sample points. This was accomplished by correcting the scene to UTM coordinates which also were used to locate the sample transects. Chemical data for each sample point included organic carbon (easily oxidizable carbon by the method of Nelson and Sommers, 1975), free iron oxide (dithionite-citrate-bicarbonate method of Kittrick and Hope, 1963), and amorphous iron content (hydroxylamine method of Chao and Zhou, 1983). We also included the ratio of amorphous iron to organic carbon because there was an apparent inverse relationship between them (Table 1).

The organic carbon and free iron oxide data are the same as in our first semiannual report but are repeated here to show relationships to amorphous iron in surface samples. Table 2 shows the distribution of amorphous iron in some profiles from the test field. The greatest amounts of amorphous iron are found in the Bt horizons as compared to either C, BC, or A horizons. Some Ap horizons show higher values than A horizons because tillage overburden contains B material that has been moved down slope.

The chemical data, DN values, and various band ratios were examined with the program package Statistix (NH Analytical Software) in order to find the combinations of reflectance data most likely to show a relationship which would dependably separate the exposed paleosols from other soils. Table 3 shows correlation coefficients (R) and P-values for the TM bands used individually. The best chance for success at predicting organic carbon levels and amorphous iron was with TM5 and TM7. There was no good relationship with free iron oxide. Apparently there was not enough difference expressed at the soil surface of the cultivated field to differentiate it by reflectance in these single wavebands.

Better results were obtained with band ratios (Table 4). Ratios having potential for discriminating organic carbon on this site were TM 1/4, 5/4, 5/7, 5/3, 5/2, 4/7, 3/5, 3/7, 4/1, and 4/5. The best candidates to

discriminate amorphous iron were 5/4, 4/7, and 4/5. The analysis suggests only marginal success for free iron oxide with 3/4, 4/3, and 5/7. Since organic carbon and amorphous iron are inversely related, the ratio of the two is best modeled with the same bands indicated for organic carbon alone.

We also looked at combinations of three bands or three ratios to predict the soil properties (Table 5). The best relationships were for organic carbon and the ratio of amorphous iron to carbon followed by amorphous iron and free iron oxide in that order.

Cluster analyses and Fastclas classification procedures were applied to the most promising of the band ratio combinations. Figure 1 shows the distribution of clusters in TM 5/3 by TM 3/4 data-space used to model the amorphous iron/organic carbon ratio. The distribution pattern shows a soil line and a group of clusters from areas of mixed plants and soil. The soil line shows a progression from a small ratio value at cluster 20 to a large value at cluster 22. There is an increase in amorphous iron from cluster 20 to 22 and a decrease in organic carbon. There is a decrease in TM5 / TM3 DN which matches the decrease in organic carbon. The soil line is mapped in Figure 2a where the print density increases with increasing carbon. The most eroded soils are well represented by the symbols -, =, and +. Figure 2a may be compared to Figure 2b, an aerial photograph taken near the time of the satellite overpass.

Figure 3 shows the cluster distribution for the best model of amorphous iron. TM band ratios 5/3, 3/1, and 4/5 were used to produce this data set and the map in Figure 4. The soil line is represented by clusters 3, 4, 5, 8, and 10 representing decreasing amounts of amorphous iron from three to 10. This produces a map similar to the one shown in Figure 2a, but with less detail. Again, the eroded soils are well represented; however, it is not clear which if any of these clusters in either data set represent B horizons from Holocene soils and which represent Bt horizons from paleosols. The exposed paleosols are well mapped but may include some of the younger soil B horizons. Final evaluation of these models cannot be carried out until the field drys later in spring.

Figures 5 and 6 show the cluster distribution and Fastclas map for organic carbon in of the same area. These were derived by using band ratios 5/4, 3/4, and 1/4. The striking similarity to the previous maps as well as the statistical data suggest that carbon is by far the most important soil property being mapped. If the small amount of iron in these soils has enough influence on reflectance to allow separation of eroded paleosols from eroded Holocene soils we have not yet found a way to do it. We feel that more conclusive evidence may be found by combining data sets from this area and from the carbonate soil area reported in our second semiannual report. The carbonate soil area had clusters to represent the carbonate-enriched paleosols, iron-enriched paleosols, and a sequence of organic carbon contents. Any clusters which are separable but which have similar low carbon values may be the ones associated with the various B horizons.

I.C. Define, on the basis of results of A and B to the extent possible, where exposed paleosols exist within fields that are not bare, but have a crop cover, and the distribution of

desirable and undesirable soil properties in each field.

We have studied this problem by using imagery from 1985, which covers the same fields that we worked on with 1984 imagery, to analyze the patterns of bare soil. On the field of interest, the 1984 summer fallow operation was followed by a winter wheat crop. Imagery for 1985 was acquired on June 15 and July 17. Thus far, we have studied the June 15 image. The crop was nearing maturity, but had not ripened. An aerial photograph taken July 1 (Figure 7) shows a complete range of colors from green in the valleys to golden brown on south-facing slopes. This photograph shows less green than was in the field on the date of the satellite overpass two weeks earlier.

We have used two techniques to study this problem, a clustering and classification routine, and principal components analysis. The chosen data set included the winter wheat field to be mapped and several adjacent fields with bare soil, spring wheat, and winter barley. Clustering was done using TM band ratios of 5/4, 3/4, and 2/4. The distribution of clusters (Figure 8) was very similar in shape to the one acquired from the 1984 data for the same area; with the exception that the June 15, 1985 scene has clouds and cloud shadows in it. The soil line forms a flat side in the upper right corner of the graph which has TM 5/4 as the y axis and TM 3/4 as the x axis. Greenness clusters are tightly grouped toward the origin. Clouds and cloud shadows fall below the triangle formed by the two ends of the soil line and the tip of greenness. By studying the Fastclas map of these clusters (Figure 9) and comparing it to an aerial photograph of the bare soil (Figure 10) and to the aerial photograph of the crop (Figure 7) we can find the locations of clusters which represent known locations of paleosol exposures or near exposures.

Clusters 24, 27, 26, and 28 in Figure 9 which form the upper right end of the greenness block of clusters are the ones which match the known locations of the paleosols. These are mapped by Fastclas with the symbols /, =, and - for clusters 24 and 27, 26, and 28, respectively (Figure 9). The pattern which forms on the map is similar to the lightest colored areas of the aerial photographs (Figures 7, 10) and to the patterns found earlier on the bare-soil field made from the 1984 data.

Principal components analysis was used based on the idea that nonuniform areas of the crop canopy would be separted because they exhibit greater variation in reflectance values. Less than complete cover by plants means that soil and plant reflectances are mixed. The analysis was run with TM bands 2, 3, 4, 5, and 7. The first three vectors accounted for 99.8% of the variance in the scene. These were printed and on visual evaluation showed that the areas of nonuniformity were associated with known locations of the paleosols. Some aspects of the paleosol patterns were visible in each of the three components so we decided to combine them using the cluster/Fastclas routine. This resulted in clusters being separated on the basis of variance. Those with high values were associated with the paleosols, roads, clouds and cloud shadows. A Fastclas map (Figure 11) is supplied for comparison to the other maps and aerial photographs.

We have not completed these analyses yet. We would like to continue with an analysis of correlation statistics to establish some degree of agreement between the images with crop cover and the images of bare soil. We would

also like to study how the ratio clusters shift in the distribution field as a result of introducing various amounts of plant cover. It is evident in Figure 8 that cluster 28 was near the equivalent position of cluster 44 at the lower end of the soil line when we analyzed the 1984 data. It would be of interest to know where the rest of the soil line would be located if partially covered with plants and plotted in TM ratio data-space. We would also like to try other kinds of image enhancement routines on the principal components and on the output from cluster and Fastclas.

References

Chao, T. T., and Liyi Zhou. 1983. Extraction techniques for selective dissolution of amorphous iron oxides from soils and sediments. Soil Sci. Soc. Am. J. 47:225-232.

Kittrick, J. A., and E. W. Hope. 1963. A procedure for the particle-size separation of soils for X-ray diffraction analysis. Soil Sci. 96:319-325.

Nelson, D. W., and L. E. Sommers. 1975. A rapid and accurate procedure for estimation of organic carbon in soils. Indiana Acad. of Sci. Proc. 84:456-462.

NH Analytical Software, 801 West Iowa Avenue, St. Paul MN 55117

Table 1. Content of organic carbon, amorphous iron, free iron oxide, and the ratio of amorphous iron to organic carbon in surface soils of the test site.

Soil Sample	Organic Carbon	Amorphous Iron	Free Iron	Am. Fe/OC
	---------- g/Kg ----------			
P1-1	13.7	3.68	5.55	26.9
2	10.2	4.51	8.03	44.2
3	7.2	6.80	8.51	94.4
4	17.5	3.91	7.70	22.3
5	15.1	3.51	8.11	23.2
6	9.1	6.49	9.18	71.3
7	12.4	5.67	7.65	45.7
8	17.2	4.50	8.88	26.2
9	14.4	3.79	6.83	26.3
10	16.7	2.92	5.92	17.5
P2-1	13.8	5.56	9.66	40.3
2	17.6	3.79	8.76	21.5
3	12.5	5.23	8.44	41.8
4	11.4	4.74	7.49	41.6
5	20.6	4.40	7.89	21.4
6	17.8	3.78	7.73	21.2
7	20.7	3.82	7.92	18.5
8	18.2	4.61	8.41	25.3
9	8.2	6.35	7.59	77.4
10	14.4	4.76	7.27	33.1
11	14.9	3.16	8.39	21.2
12	20.0	3.65	6.34	18.3
P3-1	15.7	3.31	8.25	21.1
2	14.8	4.08	7.76	27.6
3	9.7	6.28	7.73	64.7
4	12.6	5.44	9.14	43.2
5	20.5	4.19	8.40	20.4
6	17.4	4.35	6.69	25.0
7	21.4	3.45	6.31	16.1
8	12.9	3.53	8.54	27.4
9	13.3	5.15	7.78	38.7
10	17.1	3.21	6.17	18.8

Table 2. Vertical distribution of iron oxides in soils from the test site.

Horizons	Depth (cm)	Amorphous iron	Free iron
		g/kg	
Thatuna series			
Ap	0-50	4.63	8.15
A	50-63	4.55	8.35
A/B	63-115	4.53	8.93
E	115-140	5.36	8.67
Btb	140-260	5.91	9.21
Naff series			
Ap	0-24	6.17	8.45
A	24-52	5.50	7.66
BA	52-77	6.03	6.18
Btb1	77-120	7.17	9.48
btb2	120-210	7.18	8.64
Palouse seris			
A	0-35	4.29	9.55
B/E	35-40	5.57	9.60
Btb	40-100	7.44	10.81
BC	100-135	5.81	10.74
Garfield series			
Ap	0-13	5.69	9.44
Btb	13-33	8.46	10.57
C	33-87	5.14	10.50

Table 3. Comparison of R and P values for reflectance and chemical data.

TM Band		Soil Properties			
		Organic Carbon	Amorphous Iron	Free Iron Oxide	Am. Fe/OC
		g/Kg			
1 (Blue)	R	0.210	-0.271	-0.085	-0.286
	P	0.266	0.111	0.805	0.086
2 (Green)	R	-0.151	-0.085	-0.113	0.005
	P	0.504	0.805	0.684	0.999
3 (Red)	R	-0.194	-0.059	-0.160	0.064
	P	0.324	0.900	0.462	0.883
4 (IR1)	R	-0.257	0.011	-0.034	0.136
	P	0.138	0.996	0.966	0.573
5 (IR2)	R	0.398	-0.396	-0.072	-0.471
	P	0.008	0.009	0.856	0.001
7 (IR3)	R	0.538	-0.435	-0.172	-0.568
	P	0.000	0.003	0.411	0.000

Table 4. Comparison of R and P values for TM band ratios and chemical data.

TM Band Ratio		Soil Properties			
		Organic Carbon	Amorphous Iron	Free Iron Oxide	Am Fe/O C
		g/Kg			
1/4	R	0.557	-0.238	-0.032	-0.433
	P	0.000	0.182	0.969	0.003
3/4	R	0.094	-0.151	-0.323	-0.123
	P	0.768	0.506	0.043	0.637
5/4	R	0.703	-0.437	-0.046	-0.651
	P	0.000	0.003	0.939	0.000
5/7	R	-0.533	0.271	0.302	0.464
	P	0.000	0.110	0.064	0.001
5/3	R	0.538	-0.283	0.103	-0.472
	P	0.000	0.090	0.726	0.001
5/1	R	0.415	-0.366	-0.042	-0.463
	P	0.005	0.018	0.948	0.002
5/2	R	0.609	-0.372	0.034	-0.552
	P	0.000	0.015	0.966	0.000
3/1	R	-0.412	0.090	-0.184	0.278
	P	0.006	0.786	0.363	0.199
3/2	R	-0.211	0.005	-0.222	0.152
	P	0.264	0.999	0.229	0.498
4/7	R	-0.696	0.425	0.133	0.655
	P	0.000	0.004	0.589	0.000
3/5	R	-0.519	0.283	-0.085	0.464
	P	0.000	0.091	0.807	0.001
3/7	R	-0.611	0.333	0.011	0.550
	P	0.000	0.035	0.997	0.000

Table 4. Comparison of R and P values For TM Band Ratios and chemical data (continued).

TM Band Ratio		Soil Properties			
		Organic Carbon	Amorphous Iron	Free Iron Oxide	Am. Fe/OC
		g/Kg			
4/1	R	-0.531	0.203	0.024	0.403
	P	0.000	0.292	0.982	0.007
4/2	R	-0.341	0.223	0.162	0.340
	P	0.030	0.224	0.456	0.031
4/3	R	-0.098	0.173	0.307	0.155
	P	0.749	0.405	0.058	0.489
4/5	R	-0.677	0.435	0.035	0.651
	P	0.000	0.003	0.964	0.000

Table 5. Selected combinations for mapping organic carbon, amorphous iron ,free iron oxide, and ratio of Am Fe/OC.

Soil Properties	Combination (TM Bands)	R Square	P-value
Organic Carbon	1-4-7	0.562	0.000
	1/4-5/2-3/1	0.586	0.000
Amorphous Iron	3-4-5	0.300	0.011
	5/3-3/1-4/5	0.301	0.011
Free Iron Oxide	3-5-7	0.190	0.096
	5/3-3/5-4/7	0.193	0.092
Ratio of Am.Fe/OC	3-4-5	0.517	0.000
	3/4-5/4-5/3	0.524	0.000

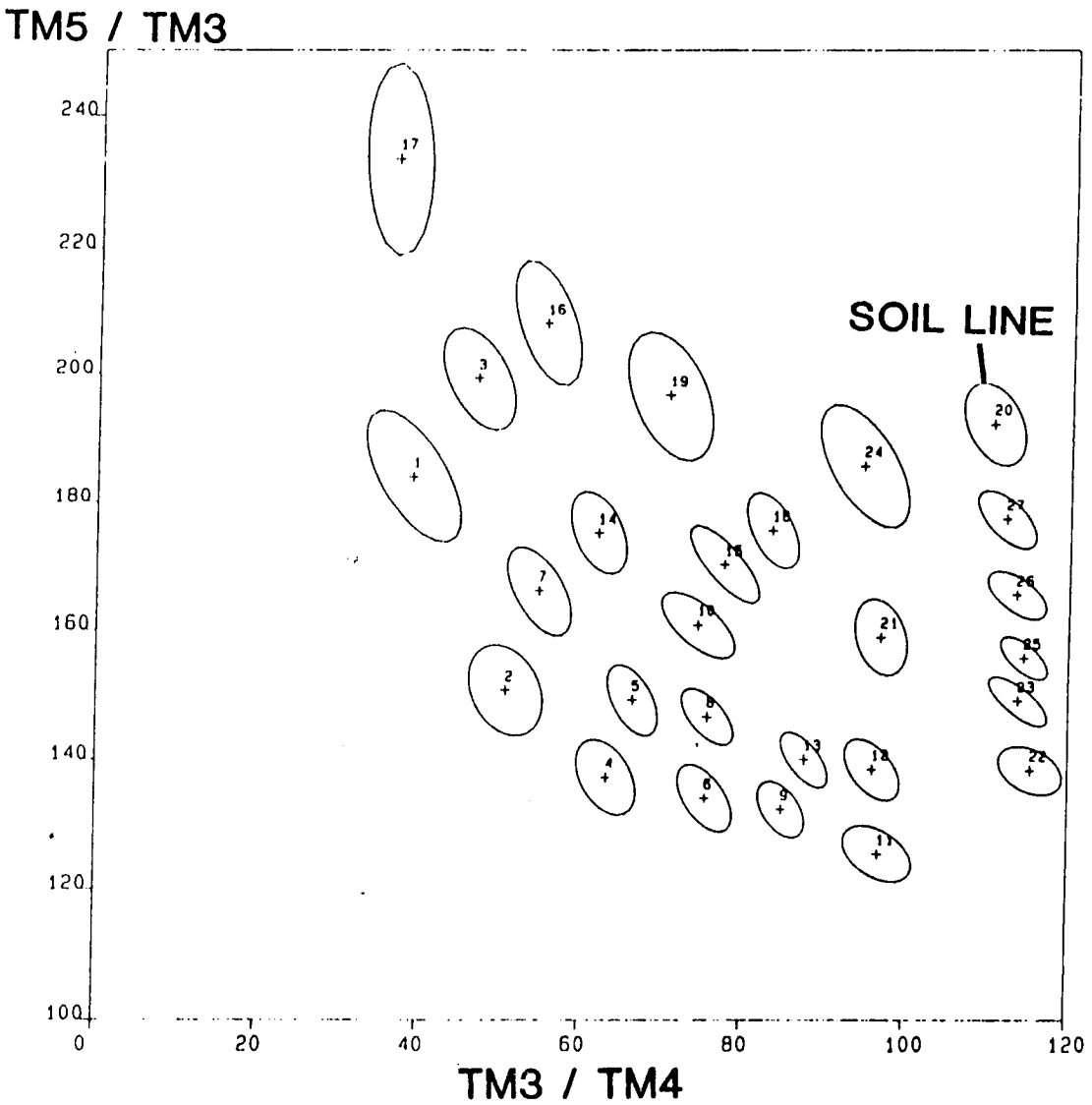

Figure 1. Plot of clusters for the Am. Fe/OC ratio model.

2a.

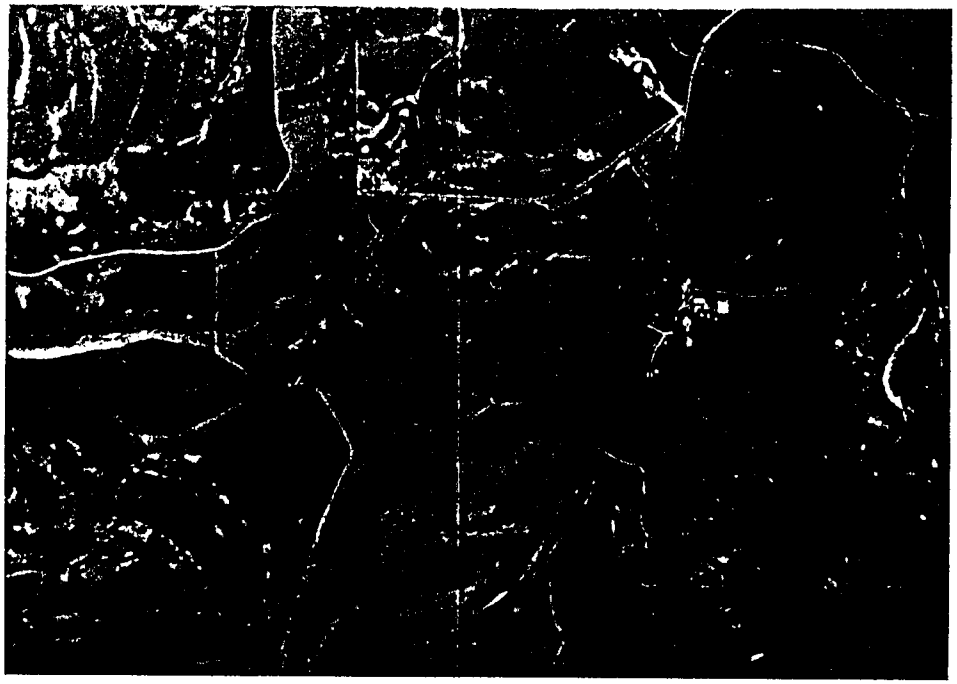

2b.

Legend

Symbol	Cluster No.	Relative Am.Fe/OC value
W	20	Smallest
$	27	
X	26	
+	25	
=	23	
-	22	Largest
P	21	Plants
P	24	Plants

Figure 2a, 2b. Model of Am. Fe/OC ratio on a bare-soil field mapped by TM ratios 3/4, 5/4, 5/3, compared to an aerial photograph taken near the time of the satellite overpass.

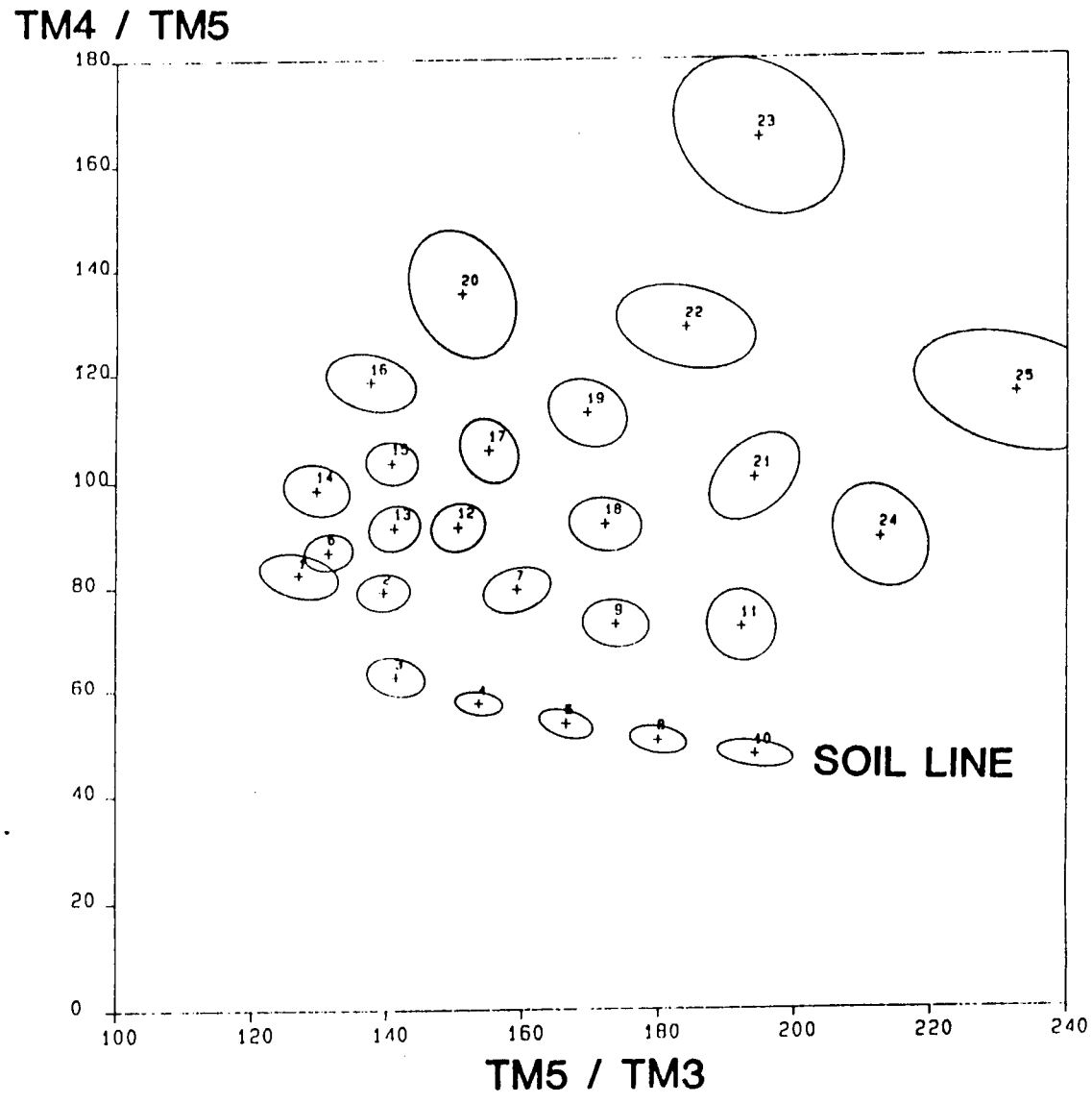

Figure 3. Plot of clusters for the amorphous iron model.

Legend

Symbol	Cluster No.	Relative Am. Fe value
-	3	Most
=	4	↑
$	5	|
Q	8	|
W	10	Least

Figure 4. Model of amorphous iron mapped by TM ratios 5/3, 3/1 and 4/5.

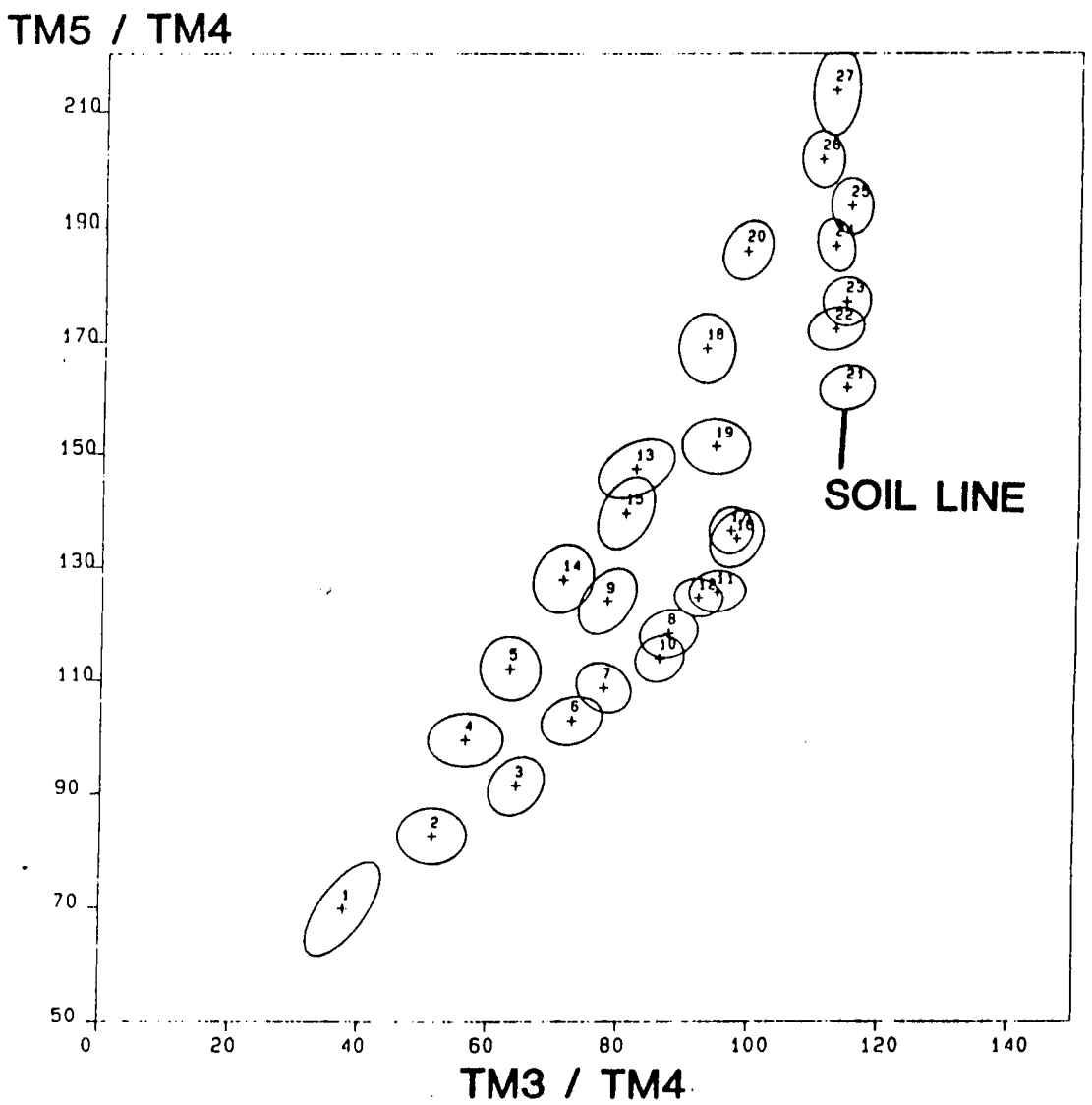

Figure 5. Plot of clusters for the organic carbon model.

Legend

Symbol	Cluster No.	Relative carbon content
-	21	Least
=	22	
+	23	
X	24	
$	25	
Q	26	
W	27	Most
P		Plants

Figure 6. Model of organic carbon using ratios 5/4, 3/4, and 1/4.

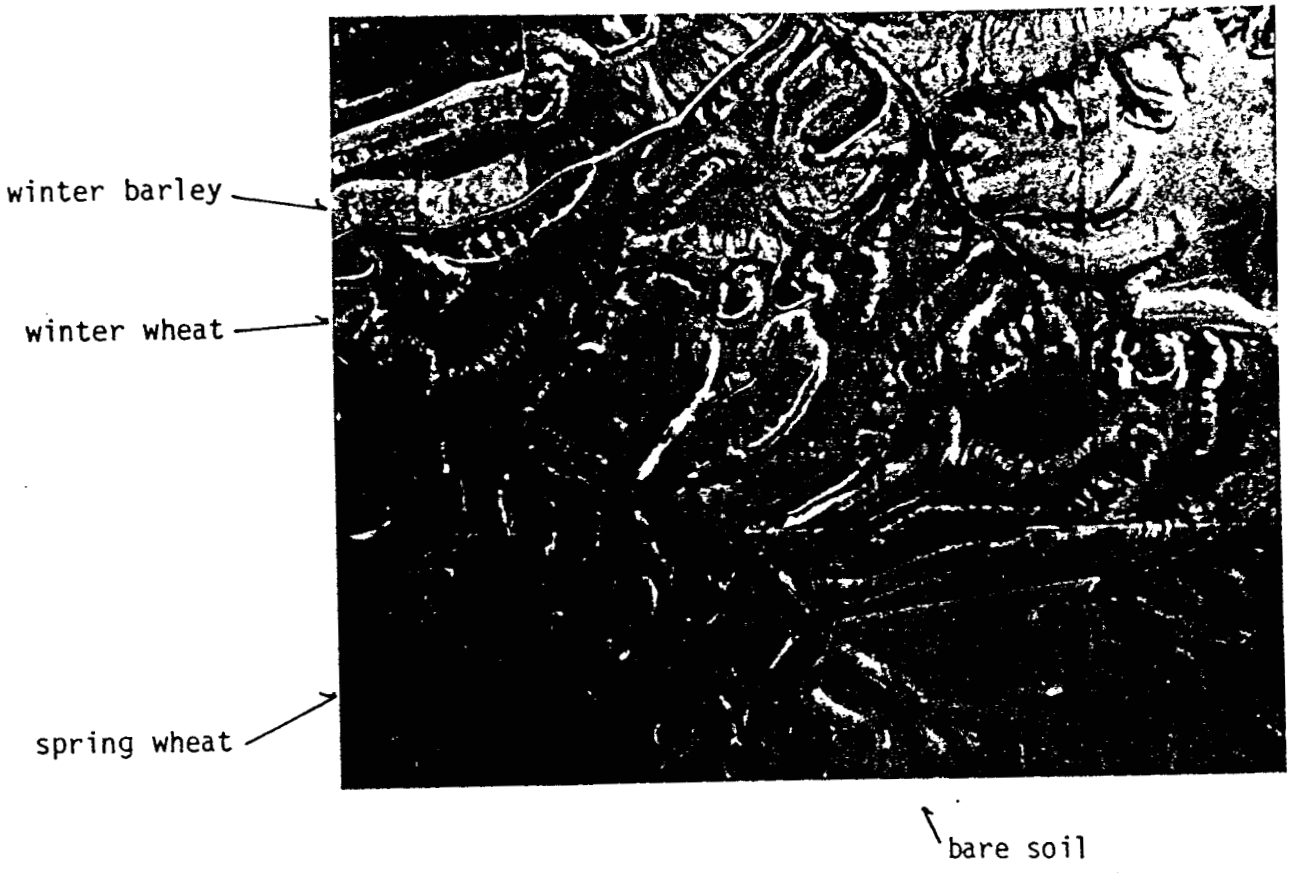

Figure 7. Ripening winter wheat field shows white color where paleosols interfere with crop growth.

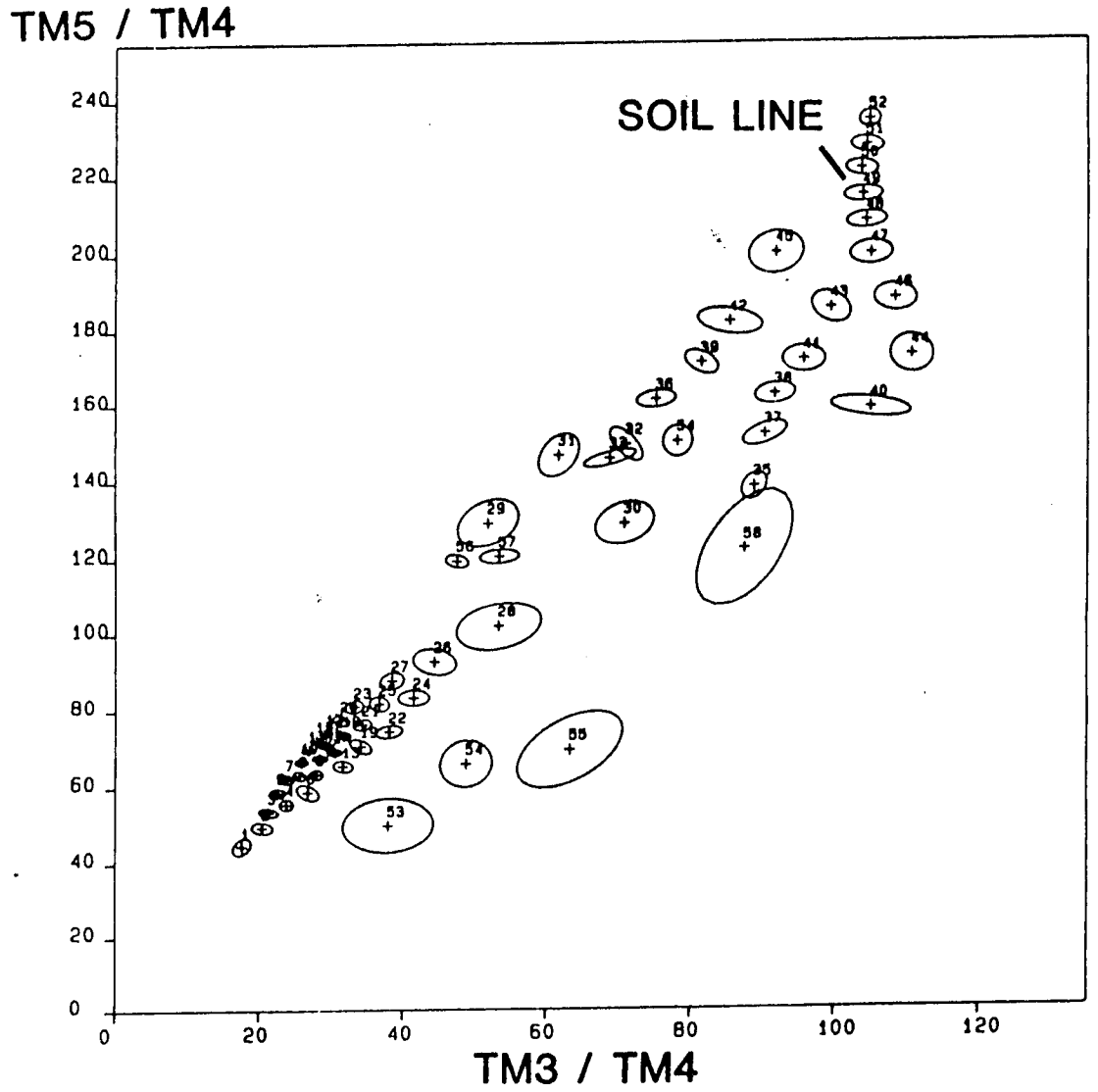

Figure 8. Plot of clusters for the model of bare soil, crops, and mixed areas.

Legend

Symbol	Cluster No.	Interpretation
-	28	Paleosols within 1 m
/	27,24	Paleosols within 1 m
=	26	Paleosols within 1 m
C	--	Clouds and cloud shadows
R	--	Ripened crop
W	--	Green crop
$,S	--	Bare soil
Blank	--	Unclassified

Figure 9. Map of winter wheat field showing areas of poor crop coverage due to the presence of exposed paleosols.

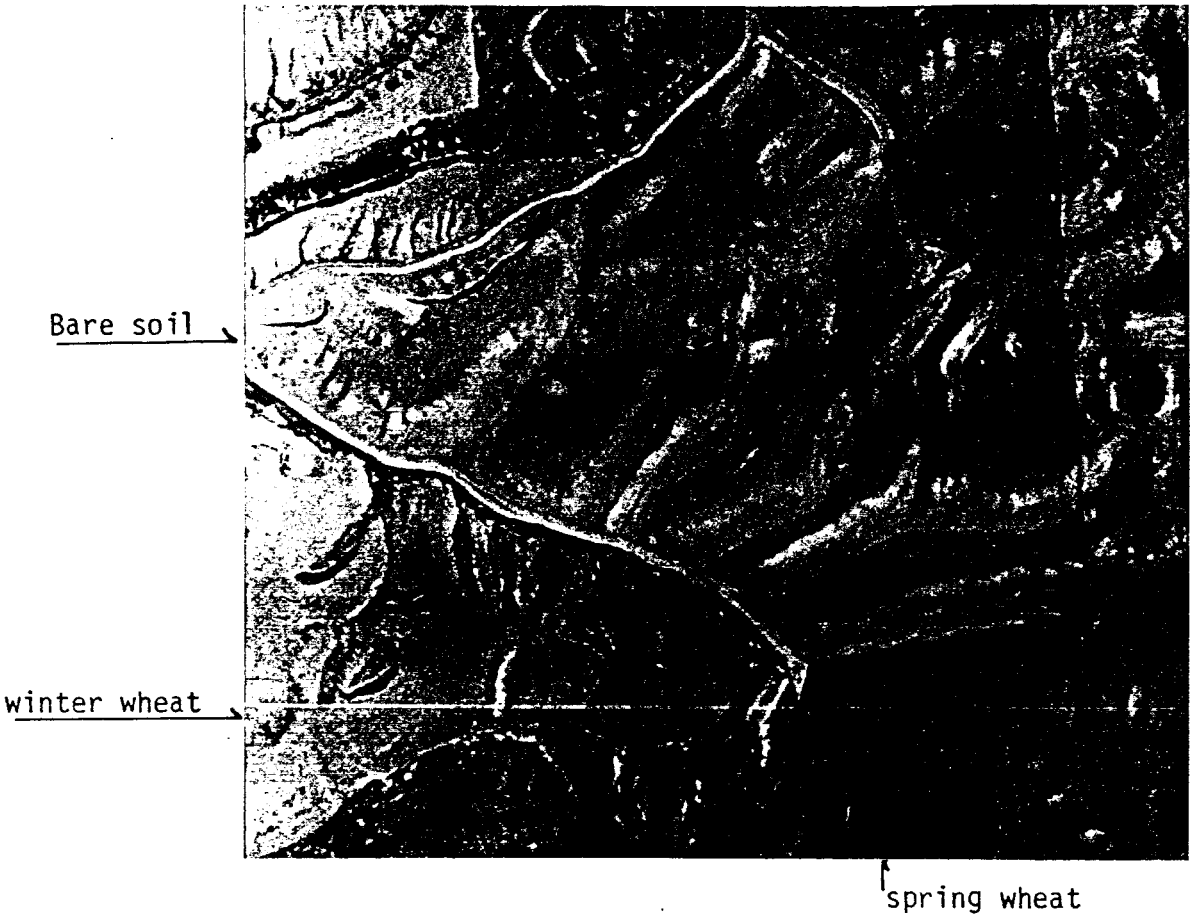

Figure 10. Aerial photograph taken July, 1984 showing the bare summer fallow field under study. Light colored areas are associated with exposures of paleosols.

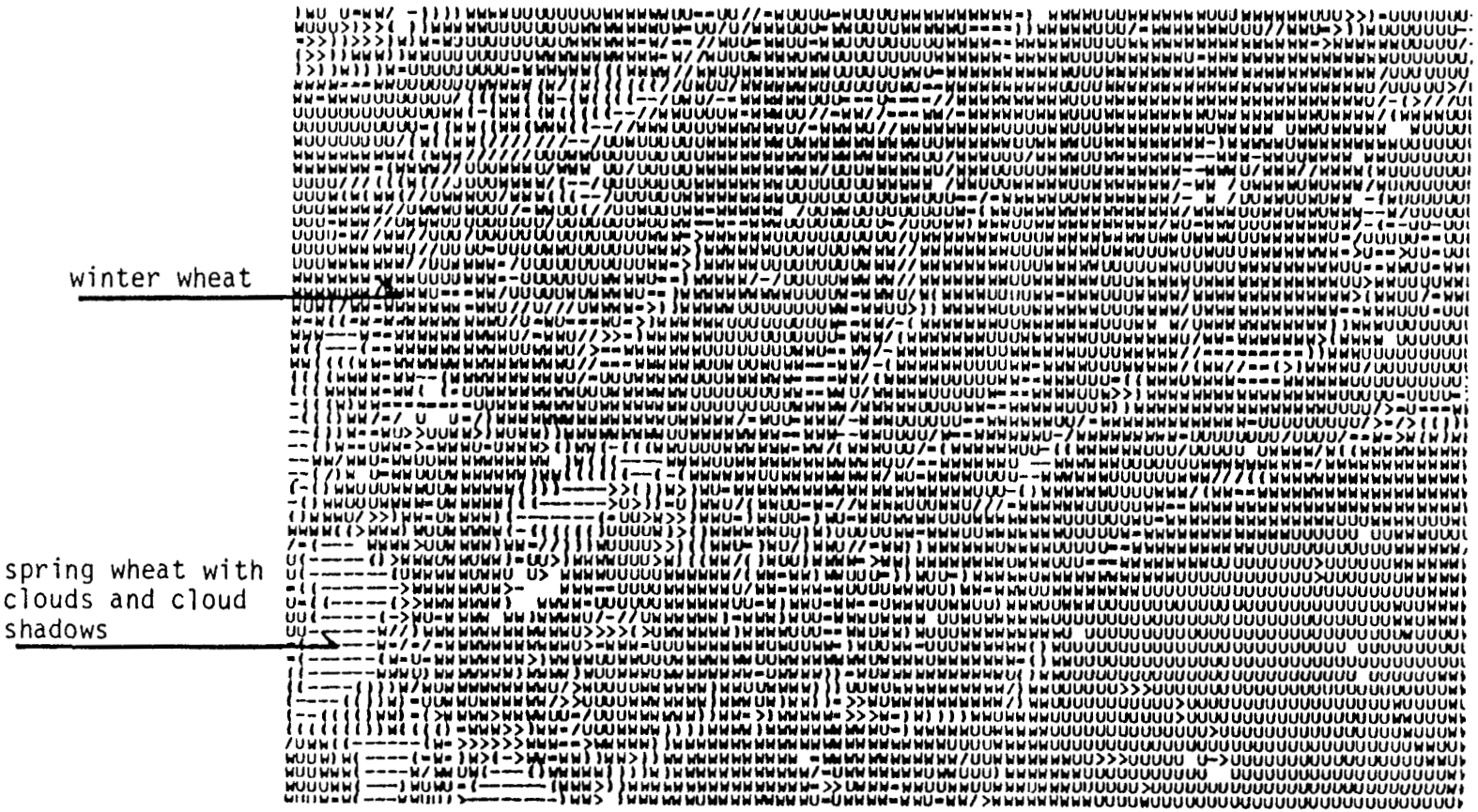

Figure 11. Fastclas map of clusters based on principal components. Light toned (high variance)